High efficiency tapered free-electron lasers with a prebunched electron beam from echo-enabled harmonic generation

Zhouyu Zhao,* Yuanfang Xu, Qika Jia, and Heting Li†

National Synchrotron Radiation Laboratory, University of Science and Technology of China, Hefei, 230029, Anhui, People's Republic of China

(Received 6 November 2022; accepted 20 June 2023; published 10 July 2023)

Undulator tapering based on a prebunched electron beam and a strong seed laser has been demonstrated as a promising method to greatly enhance free-electron laser (FEL) efficiency and suppress sideband instability. Different from the former works that introduce an ideal bunching or a seed laser or a self-seeding mechanism, in this paper, we propose to enhance FEL efficiency by optimizing the tapering strategy with a prebunched electron beam from echo-enabled harmonic generation (EEHG). The simulation results demonstrate that the efficiency enhancement can be effectively maintained in a quite long undulator, in which the whole FEL efficiency is improved by more than 2 orders and a clear center spectrum inherited from EEHG can be preserved. Benefitting from a stable initial phase space with an appropriate tapering strategy, the nature of stabilities can be well preserved at both time and frequency domain. Through jumping the resonant phase, an effective sideband suppression can be realized and the stability of output power is improved. In this scheme, the inhomogeneous shot noise and microbunching instability also have an important impact on efficiency enhancement and output stability. It shows a different instability feature from the first stage to the following tapered undulator in comparison to the self-seeding tapered scheme.

DOI: 10.1103/PhysRevAccelBeams.26.070701

I. INTRODUCTION

Generally, the free-electron laser (FEL) efficiency is limited by Pierce parameter which is typically on the level of $0.1‰ - 0.1\%$ [1]. Only a small portion of the energy is transformed from the electron beam to FEL. To enhance FEL efficiency, various methods have been put forward to extend the time duration and/or improve the speed of energy exchange. In summary, there are two different approaches: (i) directly improving the electron beam quality, such as enhancing the beam current and initial bunching, reducing the emittance and energy spread. This approach can effectively enhance FEL efficiency with several times or even higher multiple, however, its potential for efficiency enhancement is strictly limited by FEL physics and accelerator technologies. (ii) Improving FEL efficiency from the aspect of the interaction between the electron beam and FEL, which emphasizes the constraint and manipulation of electron beam and FEL, such as utilizing a helical undulator to strengthen the interaction or the undulator tapering to improve the energy exchange.

Undulator tapering is a general way to enhance FEL efficiency beyond the saturation value in the single-pass high-gain FEL [2,3]. Based on the Kroll-Morton-Rosenbluth (KMR) model, different tapering strategies have been theoretically studied or carried out in practice, such as the parabolic taper with a constant resonant phase and the specific taper determined by a variable resonant phase [3–17]. In the self-amplified spontaneous emission (SASE), through applying a weak undulator tapering, FEL power is improved by a factor of 2–4 at the x-ray region [18,19]. However, considering that SASE is started from shot noise with the growth of sideband in a long undulator, it is difficult to greatly enhance FEL efficiency in practice. In the FEL amplifier, the electron beam modulated by the seed laser brings a high FEL gain. Through utilizing a seed laser with a weak taper, FEL power is improved by several times in experiments [19–22]. Particularly, a prebunched beam with a strong seed laser can greatly enhance FEL efficiency by applying a strong taper. The theoretical studies demonstrate that the maximum efficiency has the potential to reach the ultimate limitation, which is determined by FEL resonant relation [7]. The conversion efficiency of 10%–30% has been experimentally observed by combining a strong seed laser or the superradiant emission with a strong taper at a long wavelength region [23,24]. Obviously, it is hard to obtain such a seed laser or a prebunched beam at short

*yuzz@ustc.edu.cn
†liheting@ustc.edu.cn

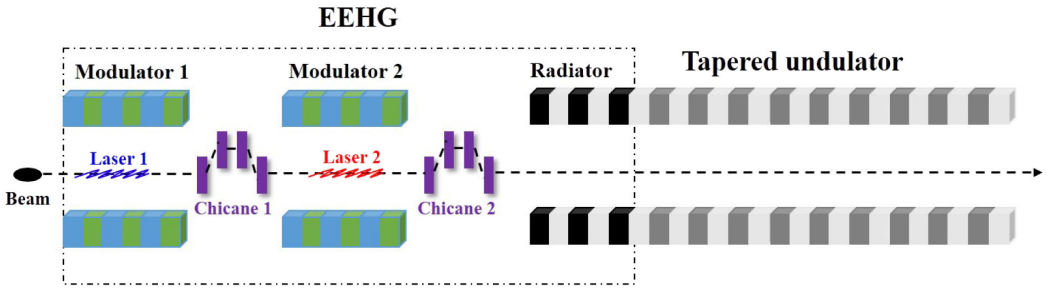

FIG. 1. Schematic of EEHG enabled high efficiency tapered FEL.

wavelength region. A promising scheme based on self-seeding mechanism has been proposed to improve FEL power to the level of terawatt at the x-ray region [9,10].

The high-gain harmonic generation, as another fundamental operation mode of FEL, has an obvious advantage in improving the longitudinal coherence and stability. Echo-enabled harmonic generation (EEHG) is one of the most promising schemes to form the initial bunching at a high harmonic with a small introduced energy spread [25–30]. In this paper, we propose to enhance FEL efficiency by optimizing the tapering strategy with a prebunched electron beam from EEHG, as shown in Fig. 1. Through optimizing the tapering strategy in the so-called postsaturation regime, FEL efficiency can be greatly improved, with a good output stability. The sideband instability is observed in the proposed scheme, nevertheless, a clear center spectrum inherited from EEHG can be preserved.

The paper is organized as follows: Sec. II introduces the general settings and performs the three-dimensional (3D) simulations of EEHG to obtain the initial bunching and input power for the following undulator tapering. In Sec. III, we discuss the taper optimization and present the time-independent 3D simulations. Based on the optimization results, we further perform the time-dependent 3D simulations in Sec. IV. The FEL instabilities from shot noise, microbunching instability, and jitter of seed laser are studied in Sec. V. Additionally, the self-seeding based tapering scheme is demonstrated as the reference, which shows a different instability feature from the first stage to the following tapered undulator in comparison to the proposed scheme. In Sec. VI, the resonant phase jumping is employed to suppress the sideband instability and improve the power stability. Finally, we make the discussion and summary.

II. INITIAL BUNCHING AND INPUT LASER FROM EEHG

A typical schematic of EEHG is shown in the left part of Fig. 1. The electron beam is manipulated by two seed lasers with two modulators and two magnetic chicanes. Assuming that these two seed lasers have the same wavelength for a specific high harmonic order $a = m + n$, the bunching factor of EEHG is given as

$$b_{n,m} = e^{-(1/2)[nB_1+(m+n)B_2]^2}|J_m[-(m+n)A_2B_2] \times J_n\{-A_1[nB_1+(m+n)B_2]\}|, \quad (1)$$

where n and m are integers, $A_1 = \Delta E_1/\sigma_E$ and $A_2 = \Delta E_2/\sigma_E$ are the energy modulation amplitudes, $B_1 = R_{56}^{(1)}k\sigma_E/E_0$ and $B_2 = R_{56}^{(2)}k\sigma_E/E_0$ are the dimensionless momentum compactions of chicanes, k is wave number, σ_E is energy spread, and E_0 is beam energy.

The EEHG-related parameters given in Table I are referenced to Shanghai Soft X-ray FEL User Facility [31,32]. The target radiation wavelength is set to the 20th harmonic (13.5 nm) of 270 nm seed lasers with $n = -1$ and $m = 21$. The modulation amplitudes A_1 and A_2 are set to about 2.8 and 2.4, respectively. Here, we scan the dispersion strengths of two chicanes to optimize the bunching factor at 20th harmonic, as shown in Fig. 2. There are two adjacent regions that can achieve the optimal $b_{n,m}$. Obviously, a small R_{56} should be beneficial to FEL performance, therefore the left region is preferred. The maximum $b_{n,m}$ greater than 0.11 can be achieved around $R_{56}^{(1)} = 5.4$ mm and $R_{56}^{(2)} = 0.286$ mm.

To verify the optimal prediction settings, we perform the 3D simulations by using *Genesis* code [33]. Figure 3 shows

TABLE I. Main parameters utilized in EEHG simulations.

Parameter	Value	Unit
Beam energy E_0	1.4	GeV
Energy spread σ_E	100	keV
Normalized emittance ε_n	1.5	mm mrad
Beam current I	1000	A
Full length l_e	100	μm
Wavelength of seed laser	270	nm
Laser power P_1, P_2	33.2, 81.7	MW
Modulation amplitude A_1, A_2	2.8, 2.4	⋯
Dispersion $R_{56}^{(1)}$, $R_{56}^{(2)}$	5.429, 0.287	mm

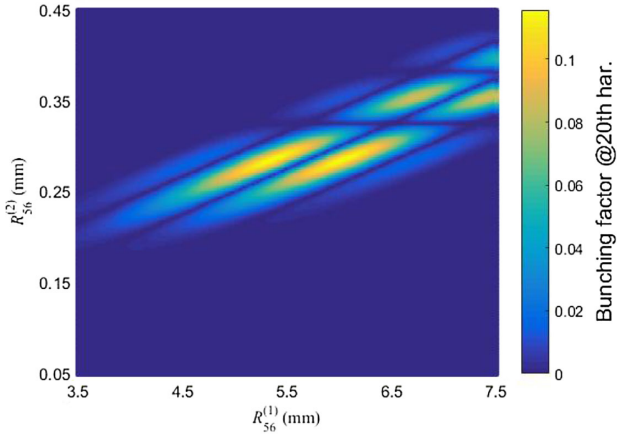

FIG. 2. Bunching factor of EEHG at 20th harmonic of 270 nm lasers at different $R_{56}^{(1)}$ and $R_{56}^{(2)}$, with $n = -1$ and $m = 21$, $A_1 = 2.8$ and $A_2 = 2.4$.

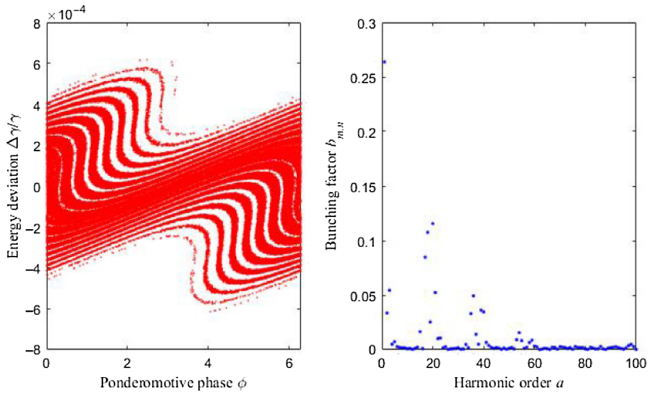

FIG. 3. Phase space (left) and bunching factor (right) after the second chicane and before the radiator.

the phase space and bunching factor after the second chicane and before the radiator. In the time-independent simulation, $b_{-1,21}$ is optimized to 0.11 with $R_{56}^{(1)} = 5.429$ mm and $R_{56}^{(2)} = 0.287$ mm, thus it is highly consistent with the theory prediction. In the following radiator of a normal EEHG configuration, the saturation power can reach more than 2 GW while the bunching factor is increased from 0.1 to 0.7. The bunching factor achieves its maximum earlier than saturation. After saturation, FEL reaches the postsaturation regime. Most of the undulator tapering strategies are focused on this regime which allows to further enhance FEL efficiency. As pointed in the previous studies on undulator tapering, the prebunched beam is especially beneficial for strengthening the energy exchange, then enhancing FEL efficiency [7,9,10]. For the proposed scheme in this paper, the initial bunching factor and input seed laser are the outputs of a normal EEHG. We prefer to utilize the electron beam and laser at the position where the bunching factor achieves maximum. The corresponding bunching factor is about 0.73 and the input laser is about 1.8 GW at position around period number $N_u = 180$.

III. TAPER OPTIMIZATION BY TIME-INDEPENDENT 3D SIMULATIONS

The primary goal of undulator tapering is efficiency enhancement. The tapering profile can be described as

$$K(z) = K_0 \times [1 - c \times (z - z_0)^d], \tag{2}$$

where K_0 is the initial resonant undulator parameter, c is the scale coefficient, and d is the profile order, in which $d = 1$ represents the linear taper and $d = 2$ represents the parabolic taper. The tapering equation and the ponderomotive phase separatrices of the Hamiltonian equation related to electron and laser can be deduced as

$$\frac{\mathrm{d}K}{\mathrm{d}z} = -2k_u f_c K_l \sin\psi_r, \tag{3}$$

$$\eta^2 = K_l K_f [\cos\psi + \cos\psi_r + (\psi + \psi_r - \pi \mathrm{sgn}\psi_r)\sin\psi_r], \tag{4}$$

where ψ_r is the resonant phase, $\eta = (\gamma' - \gamma)/\gamma$ is the energy deviation, K_f equals to $2Kf_B/(2 + K^2)$ or $2K/(1 + K^2)$ is the K function for planar undulator or helical undulator with $f_B = J_0[K^2/2(K^2 + 2)] - J_1[K^2/2(K^2 + 2)]$ being Bessel factor, f_c equals to f_B or 1 is corresponding to planar undulator or helical undulator, $K_l = eE/m_0c^2k_s$ is the dimensionless laser field with E being the laser field amplitude, k_u and k_s being the undulator wave number and laser wave number, respectively. The tapering rate is linearly proportional to $\sin\psi_r$. With a given laser strength, a weak taper is corresponding to a small $\sin\psi_r$ and a strong taper is corresponding to a large $\sin\psi_r$. Normally, only the particle inside the ponderomotive phase space can maintain a successive loss to the laser field, i.e., FEL gain.

In the KMR model, the tapering strategy can be summarized as two different classifications. One is determined by a constant resonant phase, another employs a variable resonant phase. Tapering with a constant resonant phase is close to the parabolic taper while tapering with a variable resonant phase has various tapering strategies. Actually, the optimal tapering strategy under different initial conditions seems not to be a fixed resonant phase [2]. A well-known tapering principle for maximizing efficiency is to maintain particle trapping in the phase bucket and improve FEL power as high as possible. However, to some extent, these two features are contradictory. A weak taper is beneficial for particle trapping but leads to slow energy exchange, in contrast, a strong taper accelerates the energy exchange but leads to a fast detrapping. To obtain the optimal tapering strategy, these two features must make a compromise.

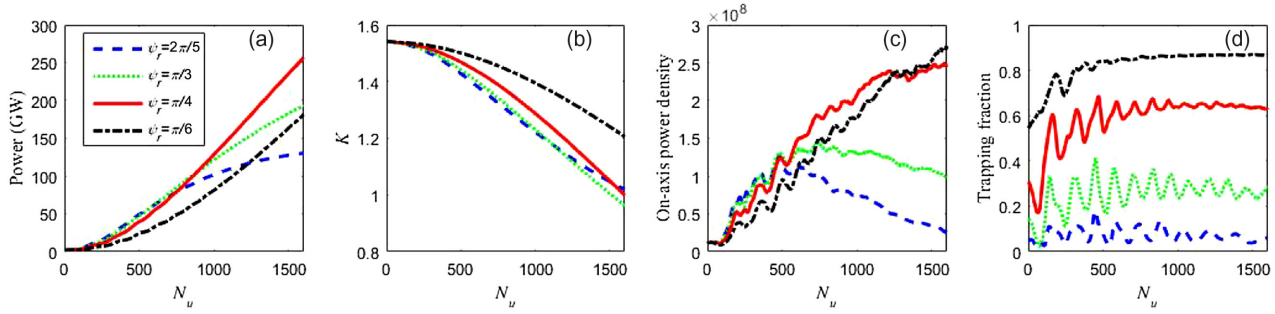

FIG. 4. Time-independent simulation with the constant resonant phase for the evolution of power (a), undulator strength parameter (b), on-axis power density (c), and trapping fraction (d) depend on undulator period number.

In a short undulator, pursuing a fast energy exchange is more preferential than particle trapping, thus a large resonant phase is better. In a long undulator, the trapping is the precondition to achieve a high efficiency. Saturation occurs until the detrapping and diffraction loss dominate the gain process. The detrapping should not be too fast, otherwise, the upper limit of efficiency enhancement will be greatly reduced. At the start stage of undulator tapering, it is preferred to maintain the trapping rather than a fast energy exchange. After FEL is amplified to some extent, a strong taper can accelerate the energy exchange and then realize a high efficiency.

In this scheme, first, we will perform the tapering strategy with a constant resonant phase, which is corresponding to the parabolic taper approximately. For the tapering with a variable resonant phase, there are various tapering strategies. Here we only limit to the simplest linear taper. To strengthen the interaction between the electron beam and FEL, we choose the helical undulator as the radiator with a period length of 6 cm. In the case of a constant resonant phase, the tapering rate is determined by the laser field and resonant phase step by step, as given in Eq. (3). Figure 4 shows the results of time-independent simulation under different resonant phase. The tapering slope with a constant resonant phase is indeed close to the parabolic line. When ψ_r is small, the power increases slowly but a high trapping fraction can be maintained. At the range of N_u from 0 to 500, FEL achieves a high power with a large ψ_r, however, the trapping fraction is small. This will lead to a slow power enhancement in the following undulator, then result in a low saturation power. In Fig. 4(c), the on-axis power density with a large ψ_r cannot maintain the growth after N_u exceeds 500, which indicates FEL gain cannot overcome the detrapping and diffraction loss anymore. It reveals that ψ_r around $\pi/4$ is corresponding to the optimal efficiency enhancement, in which FEL power is improved by 2 orders larger than the initial saturation power. The corresponding FEL efficiency reaches 18% of the electron beam, while the undulator parameter K is reduced by about 36% in the whole process. It seems that FEL power/efficiency can be further improved if the undulator length is not limited.

To make a direct comparison, we also study the linear undulator tapering, which is corresponding to a variable resonant phase. The optimal linear undulator tapering only can give about 2.5 times less power than the tapering strategy with a constant resonant phase. The strategy under a constant resonant phase seems to be more preferred than the simplest linear taper. At the start stage of FEL gain, the constant resonant phase has a smaller tapering amplitude than the linear taper but holds a better trapping fraction. After the start stage, the trapping fractions of these two cases are both around 0.6 while the former has a larger tapering amplitude than the latter. Actually, employing a large resonant phase after the start stage will be beneficial to suppressing the growth of the sideband. We will make a discussion on this point in Sec. VI.

IV. TAPER PERFORMANCE WITH TIME-DEPENDENT 3-D SIMULATIONS

The most differences between time-independent and time-dependent simulations are the slippage effect and shot noise of electron beam. In practice, it is difficult to completely overcome the slippage effect. For the tapering scheme based on SASE, the sideband can be effectively suppressed by several methods. However, the initial shot noise will introduce an unstable power strength, then the shot noise together with the intrinsic slippage effect still can arise the detrapping and limit the tapering performance. Different from the typical SASE, the high-gain harmonic generation has an initial bunching on harmonic. Though the initial harmonic bunching also amplifies the shot noise, the radiation output should be more stable than SASE. Compared with the proposed scheme, the self-seeding based tapering scheme has an unstable seed power filtered by monochromator. To some extent, the seed power is equivalent to an initial bunching factor from the perspective of FEL physics. The seed power has the function to mitigate some effects of shot noise. However, for the bunching factor at high harmonic, the effects from shot noise can be amplified by harmonic order. The instability features in these two schemes seem to be different and are dominated by different instability sources. We will discuss this point in the next section.

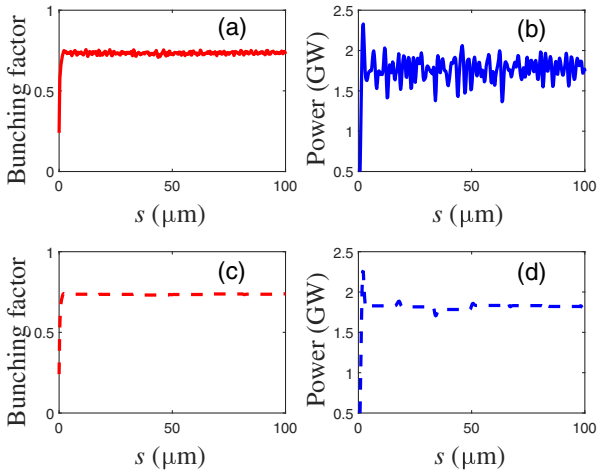

FIG. 5. Bunching factor (a, c) and output power (b, d) with time-dependent simulation before tapered undulator, in which the solid (dashed) line is corresponding to including (not including) shot noise.

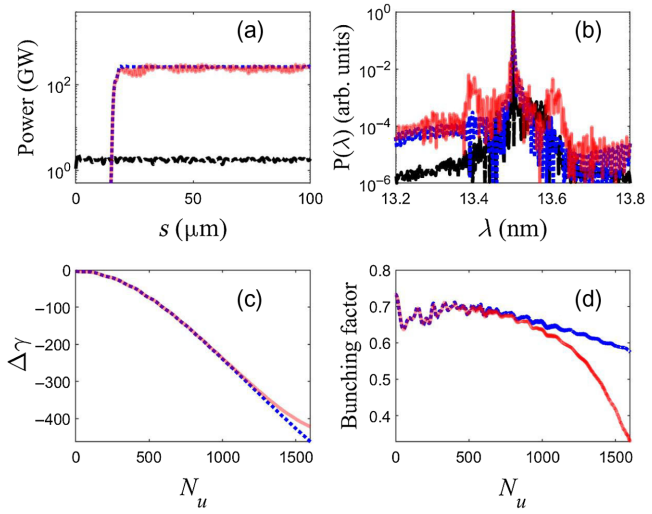

FIG. 6. Comparisons of power (a), spectrum (b), deviation of average Lorentz factor (c), and average bunching factor (d) among normal EEHG (dashed black), tapering without shot noise (dotted blue), and tapering with shot noise (solid red).

The distribution of the bunching factor and output power with time-dependent simulation before the tapered undulator is shown in Fig. 5. Here the case without shot noise is only taken as the reference and is impossible in practice. When the shot noise is turned off, the peak power in time-dependent simulation is the same as the time-independent result. If the shot noise is included, both the bunching factor and output power have an obvious fluctuation in the time domain. The time-dependent simulations with the above optimal tapering strategy ($\psi_r = \pi/4$) are shown in Fig. 6. We can find that the influence of shot noise on power enhancement is limited in time-dependent simulations. At the end of the undulator, FEL power also can be improved by more than 2 orders even considering the shot noise. It shows a good agreement with the time-independent result. Due to the synchrotron oscillation of electrons during the interaction process between FEL and electron beam, the undulator tapering slightly arises the sideband even without shot noise. Then the combination of undulator tapering and shot noise makes the spectrum suffer an obvious deterioration. For the tapering scheme based on SASE, the bunching is beneficial to suppressing sideband due to the initial chaotic spectrum, while in the proposed scheme, the initial spectrum of EEHG is clear enough, just similar to the self-seeding mechanism. Therefore, in this scheme, undulator tapering also can arise the sideband. Such an effect will gradually reduce the particle trapping, then low the final efficiency enhancement. Figure 7 shows the spectrum evolution along the undulator. The center spectrum characteristic around resonance wavelength can be well preserved, but the sideband is boosted. In the time domain, the sideband also contributes to amplifying the power fluctuation. With the growth of sideband, the time-dependent simulation with shot noise will gradually deviate from that without shot noise. Once the undulator length is further increased, this deviation will be even more obvious. The rapid detrapping finally leads to an earlier saturation than prediction.

V. INSTABILITIES

The shot noise plays an important role in a tapered undulator. To further quantify the influence of shot noise,

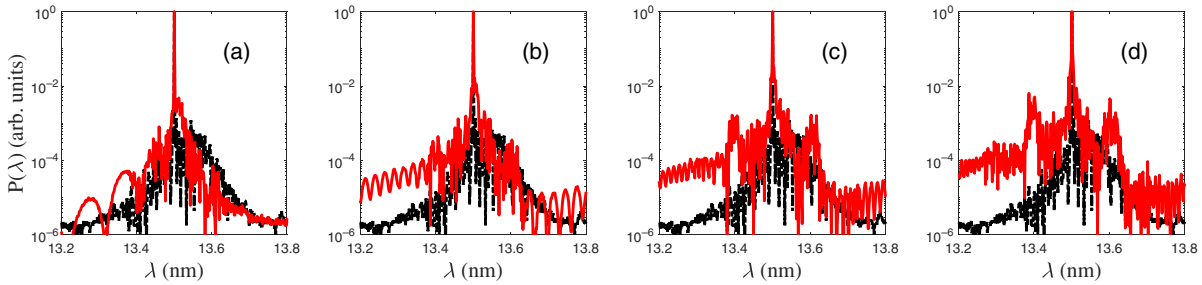

FIG. 7. Radiation spectrum (red) with shot noise at position of $N_u = 400$ (a), $N_u = 800$ (b), $N_u = 1200$ (c), and $N_u = 1600$ (d). The black line, as the reference, is the initial EEHG spectrum.

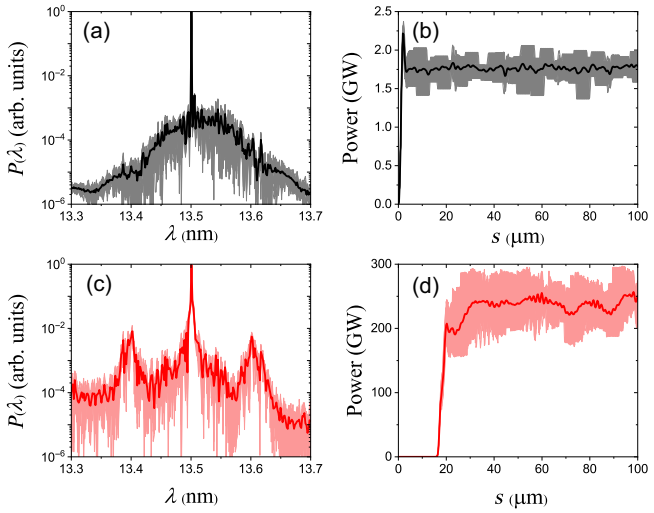

FIG. 8. Radiation spectrum (a, c) and power distribution (b, d) for a normal EEHG (upper black) and the tapered case (lower red). Thin lines refer to single shot realizations and the bold line refers to the average over 20 realizations.

we perform multiple simulations with different initial shot noise. The radiation power and spectrum are shown in Fig. 8. Actually, it is difficult to accurately represent the delicate time structure of EEHG in simulation. For an ultrahigh harmonic order, it requires amounts of particles and the simulation will become a time-consuming process. In our simulations, the number of macroparticles per slice is more than 380 000. If we increase the particle number, it is possible to further improve the stability. To demonstrate the trend on stability, the current particle number should be sufficient. The rms fluctuation of spectrum strength on resonant wavelength of a normal EEHG without tapering is about 0.2%. The normal EEHG has a stable spectrum on resonant wavelength and its power distribution varies within a certain range (rms $\sim 7\%$). In the following tapered radiator, two sidebands around resonant wavelength are amplified. The growth of the sideband makes the particle detrapping then arises the instability to some extent. The fluctuation in spectrum is 3% and the average fluctuation in power distribution is smaller than 10%, which are slightly worse than the untapered EEHG, but are still much better than FEL amplified directly from shot noise [34]. The center spectrum characteristic of EEHG is well preserved and the stability on power strength is also not deteriorated too much. The FWHM of radiation bandwidth keeps the same and the average radiation power is effectively improved by more than 2 orders. Actually, as indicated in Figs. 6–8, the efficiency can be further enhanced if we continually increase the undulator length. However, with the growth of sideband instability, the potential of efficiency enhancement will be limited. The output stabilities both at time and frequency domain are also possible to be further deteriorated.

For the proposed EEHG based tapering scheme, we can easily conclude that the stabilities at time and frequency domain are better than SASE. However, it is still not clear whether the stability in this scheme is better than a self-seeding based tapering scheme or not. Determined by the basic physics of FEL working mode, the instability from shot noise is amplified by the harmonic order in the proposed scheme. The fluctuation in phase space introduces a bunching factor instability. In contrast, FEL in self-seeding scheme works at the fundamental wavelength, the instability in physics is dominated by seed power fluctuation. To quantitatively study the stability of a self-seeding based tapering scheme as the reference, the simulations for an ideal self-seeding scheme are performed with the same parameters of the electron beam and the undulator above. A general self-seeding scheme with the fresh bunch is assumed here. Undulator tapering is also started from the position where the average bunching factor achieves maximum. The tapering profile is optimized with the average power at the entrance of the tapered undulator.

Figure 9 shows the radiation power and spectrum for a self-seeding scheme. We assume the seed laser has an average power of 5 MW and 20 seeds are uniformly distributed from 0.5 to 10 MW, which is much larger than electron beam shot noise power. The tapering profile is fixed when we vary the seed power. The case of seed laser with an ultrasmall power is neglected. For the initial self-seeding scheme, the fluctuations on power and spectrum strength are around 30% and are close to the experiment results in relevant FEL devices. The unstable seed laser deteriorates the stabilities seriously. However, after the undulator tapering, the stabilities can be greatly improved, in which the fluctuations on power and spectrum are about 4%. The tapering performance behaves insensitively to the

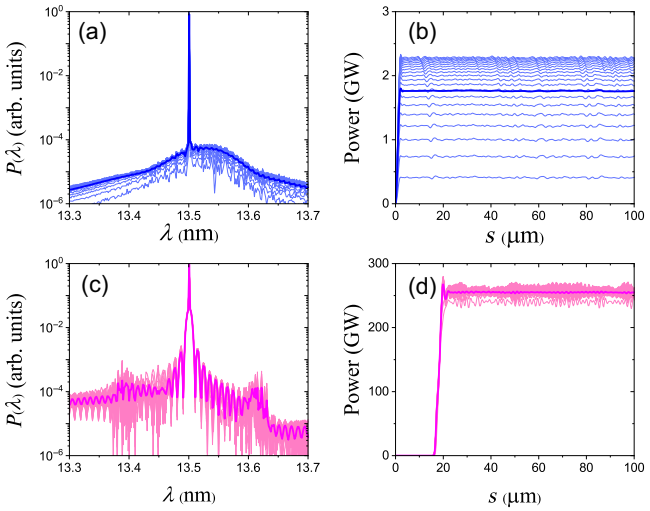

FIG. 9. Radiation spectrum (a, c) and power distribution (b, d) for a self-seeding scheme (upper blue) and the tapered case (lower magenta).

seed power fluctuation. This is benefitting from the tapering strategy with a constant resonant phase of $\pi/4$, especially at the start stage of undulator tapering. If the seed power is small, a weak taper at the start stage has little influence to FEL gain and still can make power reach saturation fast. In contrast, a large seed power will make the saturation occur before tapered undulator. However, a weak taper will make the electrons experience a slow synchrotron oscillation and cannot improve power significantly. Therefore, the fluctuation caused by seed power can be greatly reduced in this method. A similar phenomenon also can be observed in Ref. [35]. In a large range of seed power, FEL powers will be on the same level after the start stage, finally leading to a stable output.

For the self-seeding based tapering scheme, the most important instability determined by FEL physics is the seed power fluctuation. In our scheme, the most important instability determined by FEL physics is the bunching factor fluctuation. To some extent, the seed power is equivalent to an initial bunching factor, however, these two schemes still have an obvious difference in stability from the first stage to the following tapered undulator. Though the normal self-seeding scheme has an unstable output, the self-seeding based tapering scheme can still obtain a good stability, which is a great improvement than that without undulator tapering. Its power enhancement is also on the same level as the EEHG tapering scheme. Benefitting from a weaker fluctuation arisen by shot noise on fundamental harmonic than high harmonic, the self-seeding spectrum is clearer than EEHG in the tapering scheme. It leads to a result that the self-seeding stability can reach the same level or be even better than EEHG in the tapering scheme. Actually, in the proposed scheme, the stability highly depends on harmonic order. To evaluate which one can obtain a higher efficiency or a better stability, it should be discussed under the specific harmonic. In addition, the self-seeding mechanism is generally utilized from soft x-ray to hard x-ray region while EEHG is used from EUV to soft x-ray region, thus these two FEL modes should not conflict with each other.

The microbunching instability (MBI), which widely existed in linac, also has an important effect on the electron beam. For most of the harmonic upconversion schemes, MBI can be amplified and then deteriorates FEL output seriously. The laser heating system is normally used to mitigate the MBI effect. In EEHG, however, if MBI is not well suppressed, the introduced broadband energy modulation can be greatly amplified, then results in a low initial bunching factor and reduces the output stability. Obviously, in a strong tapered undulator, these effects should be carefully treated. Here we assume the electron beam has an initial density modulation, which is amplified by longitudinal space charge and can produce an energy modulation. To quantitatively study the MBI effect, the broadband energy modulation and introduced phase modulation from modulators and chicanes are summed over different frequencies, as described in Refs. [36,37]. The density modulation introduced by shot noise is normally at the level of 0.001%, while MBI can amplify the modulation by 2–3 orders of magnitude. Fortunately, with a suitable

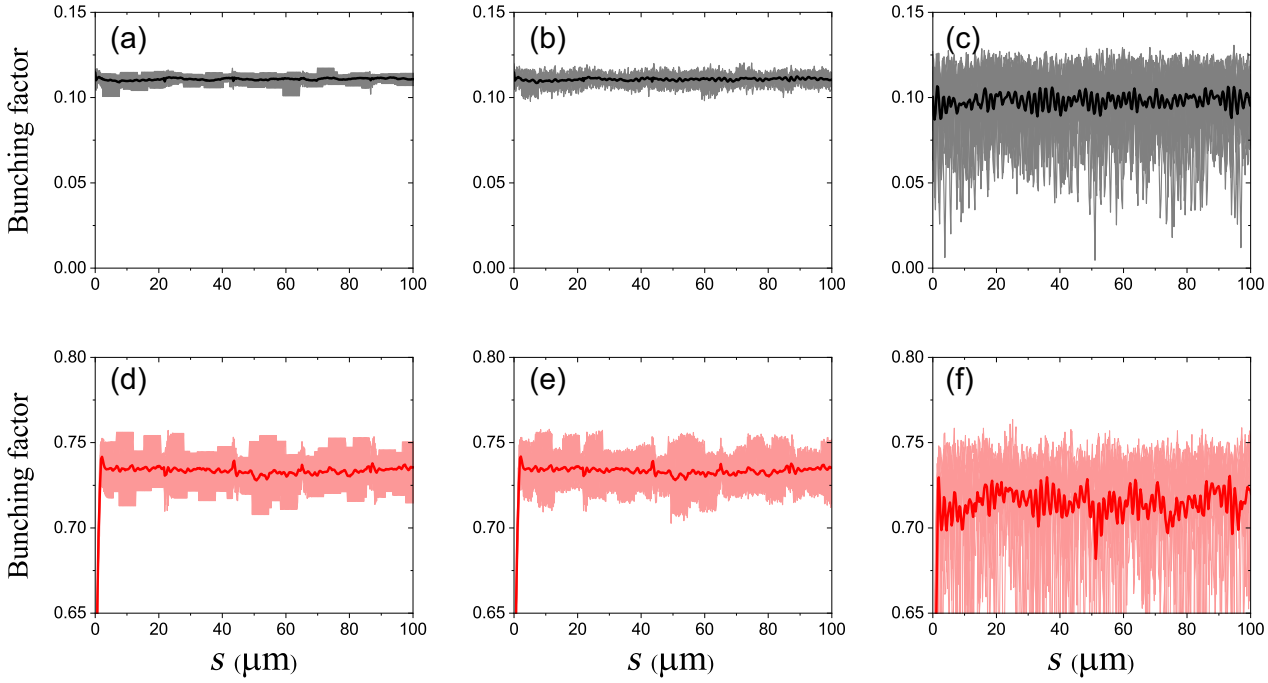

FIG. 10. Bunching factor at the entrance (upper) and exit (lower) of the first radiator, in which the left (a, d) is for only shot noise, the middle (b, e) is for density modulation of 0.01% amplitude and the right (c, f) is for density modulation of 0.1% amplitude.

laser heating system, such a modulation is possible to be mitigated to the level of 1–2 orders larger than shot noise.

To study the influence of MBI on bunching factor, we perform the numerical simulations with energy modulations and phase modulations imposed on the electron beam, as shown in Fig. 10. From the shot noise to 0.01% amplitude of density modulation, the average bunching factors at the entrance of the first radiator are almost the same, and the corresponding fluctuations are less than 2.5%. Increasing modulation amplitude to 0.1%, the decrease in average bunching factor is quite small but the fluctuation is increased to 17%. Nevertheless, due to the FEL gain and slippage effect, after the first radiator, the bunching factor instability can be mitigated to some extent. For 0.01% modulation amplitude, the average bunching factor is 0.73 and the fluctuation is about 1% at the exit of the first radiator. Increasing modulation amplitude to 0.1%, the average bunching factor is only slightly decreased to 0.71. The corresponding fluctuation is about 4.8%, which is only twice as large as shot noise. The modulation amplitude smaller than 0.1% seems to have little influence on EEHG stability. Therefore, it has a high possibility to obtain a stable output in a normal EEHG when MBI is well suppressed. However, such an influence of MBI will be amplified in the following tapered undulator, as shown in Fig. 11. The tapering profile keeps the same in the ideal case in which only shot noise is included. The influence from 0.01% modulation amplitude is almost the same as shot noise. From the shot noise to 0.1% modulation amplitude, the power fluctuation at the end of the tapered undulator is increased from 10% to 22%, while the average power is slightly decreased. The fluctuation in spectrum strength increased from 3% to 20%. Nevertheless, in this condition, FEL power is still effectively improved by nearly

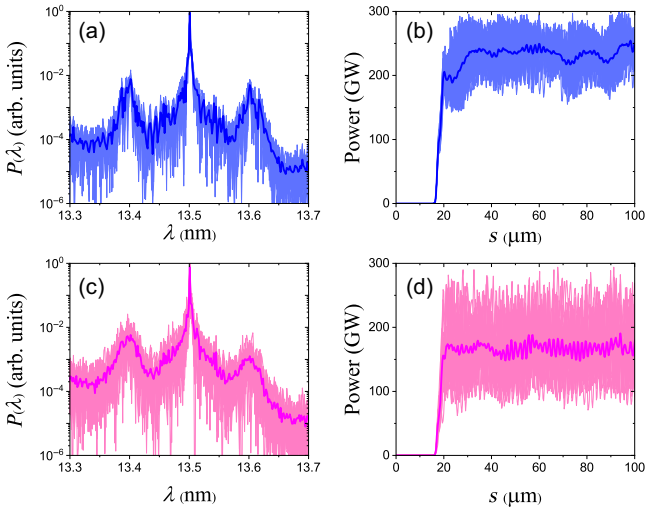

FIG. 11. Radiation spectrum (a, c) and power distribution (b, d) for a tapered EEHG with 0.01% (upper blue) and 0.1% (lower magenta) amplitude of density modulation.

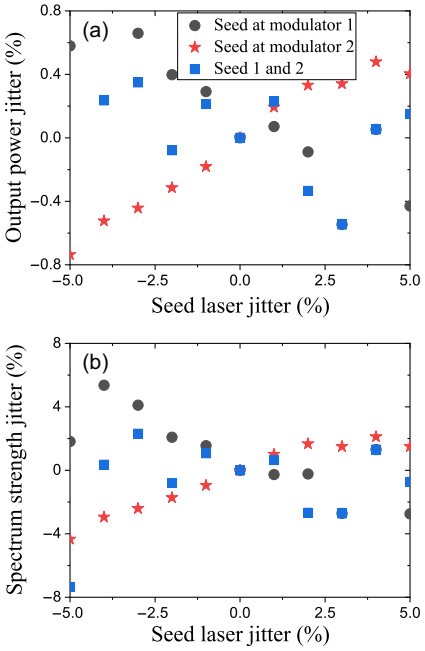

FIG. 12. Output power jitter (a) and spectrum strength jitter (b) depend on seed laser.

2 orders larger than initial power. Its stability is still much better than SASE. With a suitable laser heating system that can well suppress the density modulation, the influence of MBI on a tapered EEHG can be expected to be small. For an ultrahigh harmonic order, the tapering performance will be more sensitive to shot noise and MBI. The specific influence should be discussed and analyzed under the given harmonic order and EEHG settings.

In the proposed scheme, we also study the influence of the jitter of the seed laser on output stability, as shown in Fig. 12. It shows a good tolerance both for the seed lasers at two modulators. In the range of ±5% variation on the given seed power, the jitter of output power is always smaller than ±1%, which is greatly smaller than the fluctuation caused by shot noise. The center spectrum also can be well preserved but with a large fluctuation in spectrum strength (±7%), which is on the same level as shot noise. Therefore, the EEHG based tapering scheme is not only possible to greatly enhance FEL efficiency but also can keep a good longitudinal coherence inherited from EEHG and maintain the stable output power.

VI. SIDEBAND SUPPRESSION BY JUMPING RESONANT PHASE

Sideband suppression is an important issue in tapered undulator. Several methods have been proposed to suppress the sideband, such as introducing the phase shift to interrupt the growth of the sideband, increasing the resonant phase to speed up the synchrotron oscillation, introducing the initial bunching factor, and increasing the input power to prevent the sideband frequency from the center

frequency and reduce the influence of shot noise. In this paper, a significant sideband instability also can be found even with the initial bunching and input laser from EEHG, as shown in Fig. 8(c). The sideband shifted from the central wavelength can be quantitatively described as

$$\frac{\Delta\lambda}{\lambda} = \pm\frac{\lambda_u}{L_s} = \pm\sqrt{2K_l K_f \cos\psi_r}, \tag{5}$$

where L_s is the synchrotron oscillation period. With the increase of FEL power in a tapered undulator, the resonance between the sideband and synchrotron oscillation of the electron beam makes the particle detrapping. It will reduce the optical guiding, then lead to a roughly constant L_s and the final saturation.

The resonant phase around $\pi/4$ has been demonstrated as the optimal resonant phase to enhance FEL efficiency. Nevertheless, it seems do not yield the optimal sideband suppression, as shown in Fig. 13. When ψ_r is small, a weak sideband suppression and a strong fluctuation in output power are observed, which are similar to the self-seeding based tapering scheme [10]. Therefore, without an appropriate tapering strategy, the stability also can be deteriorated in the proposed scheme. When ψ_r is greater than $\pi/4$, a large resonant phase will further speed up the synchrotron oscillation and then suppress the sideband. The fast synchrotron oscillation with a large ψ_r leads to a rapid particle detrapping and a low saturation power but with more stable output power than a small ψ_r.

Inspired by these features at different ψ_r, in this section, we try to suppress the sideband by jumping the resonant phase before the sideband grows to a significant level. At the start stage of undulator tapering, we also keep a constant resonant phase $\psi_r = \pi/4$ to ensure the best compromise between the initial particle trapping and efficiency enhancement, then employ a large ψ_r to interrupt the fast growth of sideband in the following undulator. As shown in Fig. 7, the sideband around the center spectrum before $N_u = 1000$ does not have a significant growth, therefore, we choose to jump the resonant phase at $N_u = 800$. The phase jump is preliminary optimized from $\pi/4$ to $\pi/3$. Obviously, the tapering amplitude in phase jump is larger than a constant resonant phase of $\pi/4$. Figure 14 shows the corresponding radiation performance.

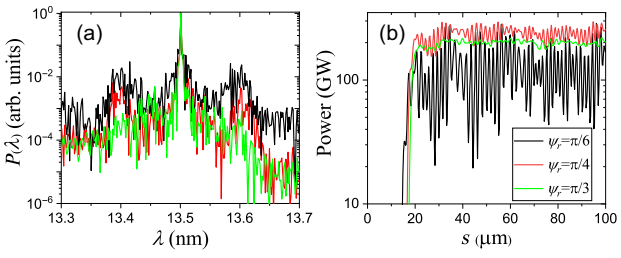

FIG. 13. Spectrum (a) and power distribution (b) with different resonant phase.

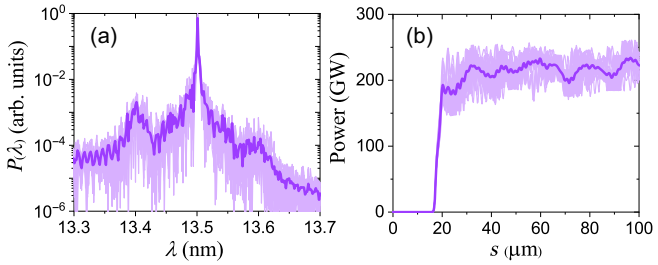

FIG. 14. Radiation spectrum (a) and power distribution (b) with the resonant phase jumping from $\pi/4$ to $\pi/3$.

Compared with a constant resonant phase of $\pi/4$, it yields an effective sideband suppression around the center spectrum, which is also beneficial to improving the stability in time domain. The average rms fluctuation of power distribution (~7%) is improved to be the same with the untapered EEHG, while the power enhancement is almost the same.

In this method, the sideband suppression is only realized by tapering the undulator parameter with a jumping resonant phase. The additional phase shifts are not employed inside the tapered undulator, thus this method should be applicable to the other tapering schemes that probably have different conditions.

VII. DISCUSSION AND SUMMARY

This paper proposes an EEHG based tapering scheme to obtain a high efficiency FEL. First, we perform a typical EEHG scheme to form the initial bunching and obtain the input power for undulator tapering. Then tapering with a constant resonant phase (closing to parabolic taper) and with the simplest variable resonant phase (linear taper) are discussed in details. It indicates that a constant resonant phase around $\pi/4$ is preferred in these two specific tapering strategies. Based on the tapering profile optimized by the time-independent 3D simulations, we perform the time-dependent 3D simulations to study some time-dependent effects. Note that the tapering profile obtained from time-independent optimization probably does not yield the highest efficiency when time-dependent effects are included, as demonstrated in Ref. [9]. In this paper, the primary goal is to try to evaluate the radiation performance of the proposed scheme at both time and frequency domain, but not just limited to finding the best tapering profile.

In the time-dependent simulations, FEL efficiency still can be improved by more than 2 orders in comparison to the initial saturation power of EEHG. The radiation performance can inherit the advantages of EEHG, then ensure a stable output. It shows a good tolerance on shot noise and jitter of seed laser. We further compare the proposed scheme with a self-seeding based tapering scheme. The normal self-seeding scheme has an unstable output, however, its output stability is possible to be greatly improved by undulator tapering. In the proposed scheme, the output

stability has slightly deteriorated from the origin, which is in contrast to the self-seeding scheme. The difference between these two FEL modes comes from the different features, in which the bunching factor fluctuation arisen by shot noise is amplified in proposed scheme while the seed power fluctuation can be greatly mitigated in the self-seeding scheme. At a high harmonic order, the bunching factor fluctuation in this scheme seems to have a stronger impact on causing instability than the seed power fluctuation in self-seeding scheme. An elaborate study on stability improvement of a self-seeding based tapering scheme will be carried on in our future works. The MBI effect in the proposed scheme is also studied in detail. With a well-suppressed MBI effect, the bunching factor fluctuation can keep small and a stable output is obtained. In addition, the center spectrum around resonant wavelength can be well preserved but the sideband instability has arisen to some extent. To suppress the sideband, we develop an easy method by jumping the resonant phase. The sideband can be effectively suppressed and the power stability is improved to be the same as a normal EEHG.

The proposed scheme shows a good potential to greatly enhance FEL efficiency in an EEHG device. In the normal high-gain harmonic generation, it should be suitable at a low harmonic but probably cannot work well at a high harmonic due to a large introduced energy spread and/or a small initial bunching. Additionally, several issues also should be carefully taken into account, such as the inhomogeneous distributions of slice current and energy spread, the mismatch between FEL and electron beam, and the energy chirp along electron bunch. These factors are also possible to deteriorate the efficiency enhancement and arise the sideband instability. Achieving a high efficiency at a high-gain short-wavelength FEL, in practice, will require more delicate studies. Studies on high efficiency tapered FEL with more practical situations will be carried on in our future works.

ACKNOWLEDGMENTS

We would like to acknowledge Dr. Pietro Musumeci at UCLA and Dr. Claudio Emma at SLAC for sharing the tapering codes on Github, and our referees for the helpful comments on MBI effect amplified by EEHG and the comparison with respect to a self-seeding based tapering scheme. We also would like to acknowledge Dr. Biaobin Li at USTC for helpful discussion on MBI. This work is supported by the National Natural Science Foundation of China under Grants (No. 11905221 and No. 11975233) and Youth Innovation Promotion Association CAS, China (No. 2020456).

[1] R. Bonifacio, C. Pellegrini, and L. Narducci, Collective instabilities and high-gain regime in a free electron laser, Opt. Commun. **50**, 373 (1984).

[2] N. Kroll, P. Morton, and M. Rosenbluth, Free-electron lasers with variable parameter wigglers, IEEE J. Quantum Electron. **17**, 1436 (1981).

[3] W. Fawley, Three plus decades of tapered undulator FEL physics, in *Proceedings of 37th International Free Electron Laser Conference, FEL2015, Daejon, Korea* (JACoW, Geneva, Switzerland, 2015).

[4] Z. Huang and G. Stupakov, Free electron lasers with slowly varying beam and undulator parameters, Phys. Rev. ST Accel. Beams **8**, 040702 (2005).

[5] E. Saldin, E. Schneidmiller, and M. Yurkov, Self-amplified spontaneous emission FEL with energy-chirped electron beam and its application for generation of attosecond x-ray pulses, Phys. Rev. ST Accel. Beams **9**, 050702 (2006).

[6] Y. Jiao, J. Wu, Y. Cai, A. W. Chao, W. M. Fawley, J. Frisch, Z. Huang, H.-D. Nuhn, C. Pellegrini, and S. Reiche, Modeling and multidimensional optimization of a tapered free electron laser, Phys. Rev. ST Accel. Beams **15**, 050704 (2012).

[7] J. Duris, A. Murokh, and P. Musumeci, Tapering enhanced stimulated superradiant amplification, New J. Phys. **17**, 063036 (2015).

[8] H. Li and Q. Jia, Optimization of single-step tapering amplitude and energy detuning for high-gain FELs, Chin. Phys. C **39**, 018101 (2015).

[9] C. Emma, K. Fang, J. Wu, and C. Pellegrini, High efficiency, multiterawatt x-ray free electron lasers, Phys. Rev. Accel. Beams **19**, 020705 (2016).

[10] C. Emma, N. Sudar, P. Musumeci, A. Urbanowicz, and C. Pellegrini, High efficiency tapered free-electron lasers with a prebunched electron beam, Phys. Rev. Accel. Beams **20**, 110701 (2017).

[11] J. Wu, N. Hu, H. Setiawan *et al.*, Multi-dimensional optimization of a terawatt seeded tapered Free Electron Laser with a Multi-Objective Genetic Algorithm, Nucl. Instrum. Methods Phys. Res., Sect. A **846**, 56 (2017).

[12] A. Mak, F. Curbis, and S. Werin, Phase jump method for efficiency enhancement in free-electron lasers, Phys. Rev. Accel. Beams **20**, 060703 (2017).

[13] J. Duris, P. Musumeci, N. Sudar, A. Murokh, and A. Gover, Tapering enhanced stimulated superradiant oscillator, Phys. Rev. Accel. Beams **21**, 080705 (2018).

[14] C.-Y. Tsai, J. Wu, C. Yang, M. Yoon, and G. Zhou, Single-pass high-gain tapered free-electron laser with transverse diffraction in the postsaturation regime, Phys. Rev. Accel. Beams **21**, 060702 (2018).

[15] Z. Y. Zhao, Y. Xu, H. Li, and Q. Jia, Efficiency enhancement of free-electron laser oscillator by kicking the electron beam orbit in a transverse gradient undulator, Nucl. Instrum. Methods Phys. Res., Sect. A **1024**, 166086 (2022).

[16] E. Schneidmiller and M. Yurkov, Optimization of a high efficiency free electron laser amplifier, Phys. Rev. ST Accel. Beams **18**, 030705 (2015).

[17] A. Mak, F. Curbis, and S. Werin, Model-based optimization of tapered free-electron lasers, Phys. Rev. ST Accel. Beams **18**, 040702 (2015).

[18] W. M. Fawley, Z. Huang, K.-J. Kim, and N. A. Vinokurov, Tapered undulators for SASE FELs, Nucl. Instrum. Methods Phys. Res., Sect. A **483**, 537 (2002).

[19] D. Ratner, A. Brachmann, F. Decker *et al.*, FEL gain length and taper measurements at LCLS, in *Proceedings of 31st International Conference, FEL'09, Liverpool, UK* (JACoW, Geneva, Switzerland, 2009).

[20] X. J. Wang, H. P. Freund, D. Harder, W. H. Miner, J. B. Murphy, H. Qian, Y. Shen, and X. Yang, Efficiency and Spectrum Enhancement in a Tapered Free-Electron Laser Amplifier, Phys. Rev. Lett. **103**, 154801 (2009).

[21] C. Emma, A. Lutman, M. W. Guetg, J. Krzywinski, A. Marinelli, J. Wu, and C. Pellegrini, Experimental demonstration of fresh bunch self-seeding in an X-ray free electron laser, Appl. Phys. Lett. **110**, 154101 (2017).

[22] I. Inoue, T. Osaka, T. Hara *et al.*, Generation of narrow-band X-ray free-electron laser via reflection self-seeding, Nat. Photonics **13**, 319 (2019).

[23] N. Sudar, P. Musumeci, J. Duris *et al.*, High Efficiency Energy Extraction from a Relativistic Electron Beam in a Strongly Tapered Undulator, Phys. Rev. Lett. **117**, 174801 (2016).

[24] A. Fisher, Y. Park, M. Lenz, A. Ody, R. Agustsson, T. Hodgetts, A. Murokh, and P. Musumeci, Single-pass high-efficiency terahertz free-electron laser, Nat. Photonics **16**, 441 (2022).

[25] G. Stupakov, Using the Beam-Echo Effect for Generation of Short-Wavelength Radiation, Phys. Rev. Lett. **102**, 074801 (2009).

[26] D. Xiang and G. Stupakov, Echo-enabled harmonic generation free electron laser, Phys. Rev. ST Accel. Beams **12**, 030702 (2009).

[27] D. Xiang, E. Colby, M. Dunning *et al.*, Demonstration of the Echo-Enabled Harmonic Generation Technique for Short-Wavelength Seeded Free Electron Lasers, Phys. Rev. Lett. **105**, 114801 (2010).

[28] Z. T. Zhao, D. Wang, J. Chen *et al.*, First lasing of an echo-enabled harmonic generation free-electron laser, Nat. Photonics **6**, 360 (2012).

[29] E. Hemsing, G. Stupakov, D. Xiang, and A. Zholents, Beam by design: Laser manipulation of electrons in modern accelerators, Rev. Mod. Phys. **86**, 897 (2014).

[30] P. Ribic, A. Abrami, L. Badano *et al.*, Coherent soft x-ray pulses from an echo-enabled harmonic generation free-electron laser, Nat. Photonics **13**, 555 (2019).

[31] Zhentang Zhao, Dong Wang, Qiang Gu, Lixin Yin, Ming Gu, Yongbin Leng, and Bo Liu, Status of the SXFEL Facility, Appl. Sci. **7**, 607 (2017).

[32] N. Huang, H. Deng, B. Liu *et al.*, Features and futures of x-ray free-electron lasers, Innovation **2**, 100097 (2021).

[33] S. Reiche, GENESIS 1.3: A fully 3D time-dependent FEL simulation code, Nucl. Instrum. Methods Phys. Res., Sect. A **429**, 243 (1999).

[34] E. Saldin, E. Schneidmiller, and M. Yurkov, Statistical properties of radiation from VUV and X-ray free electron laser, Opt. Commun. **148**, 383 (1998).

[35] G. Geloni, V. Kocharyan, and E. Saldin, A novel self-seeding scheme for hard X-ray FELs, J. Mod. Opt. **58**, 1391 (2011).

[36] E. Hemsing, Bunching phase and constraints on echo enabled harmonic generation, Phys. Rev. Accel. Beams **21**, 050702 (2018).

[37] N. S. Mirian, G. Perosa, E. Hemsing *et al.*, Characterization of soft x-ray echo-enabled harmonic generation free-electron laser pulses in the presence of incoherent electron beam energy modulations, Phys. Rev. Accel. Beams **24**, 080702 (2021).